Organic Polymer Light-Emitting Devices on a Flexible Plastic Substrate

Jerzy Kanicki,[a,b] Shu-Jen Lee,[b] Yongtaek Hong,[a] and Chia-Chen Su[a]

a) Organic and Molecular Electronics Laboratory, Department of Electrical Engineering and Computer Science, University of Michigan, Ann Arbor, Michigan, USA

b) Macromolecular Sci. & Engin. Center, University of Michigan, Ann Arbor, Michigan, USA

Phone : 734-936-0964 , E-mail : kanicki@eecs.umich.edu

Abstract

We report on the opto-electronic properties of red, green, and blue poly (fluorene) co-polymer light-emitting devices (PLEDs) fabricated on a flexible plastic substrate. The plastic substrate used has a multi-layer structure with water vapor and oxygen transmission rates of less than 10^{-5} g/cm^2-day-atm and 10^{-7} cc/cm^2-day-atm, respectively. We obtained a wide range of color gamut and a maximum emission efficiency of 0.7, 10, and 1.7 cd/A for red, green, and blue PLEDs, respectively. Finally, a simple equivalent circuit model is proposed to simulate PLED current density-voltage characteristics.

1. Introduction

Flexible displays are one of the most attractive trends in flat panel display technology. Especially, active-matrix organic light-emitting displays (AM-OLEDs) technology is one of the most promising candidates for high-definition, flexible, flat panel displays (FPDs) [1] since OLEDs have the advantages of low power consumption, high brightness and contrast, broad color gamut, wide viewing angle, potential low manufacturing cost at low temperature, and easy integration with flexible substrates. Recently, several groups have demonstrated passive matrix [2],[3] and active matrix [4] OLED displays on plastic substrates.

The good candidates for flexible substrate materials are polymers, metal foils, and ultrathin glass [5]. Gustafsson *et al.* [6] fabricated fully flexible polymer light-emitting diodes on poly (ethylene terephthalate) (PET) substrate in 1992. They used a polyaniline anode for their devices to overcome the brittle properties of the indium-tin-oxide (ITO). In 1997, Gu *et al.* [7] successfully demonstrated vacuum-deposited OLEDs on ITO-coated polyester substrates. They reported that the flexible OLEDs did not deteriorate after repeated bending. Recently, a fluorine-containing polyimide substrate has been used for vacuum-deposited OLED fabrication [8]. A standard sputtering method was used to deposit ITO layer, whose optical, electrical, and surface characteristics were optimized during ITO sputtering. In all three cases, the opto-electronic performance of the devices was comparable to that of OLEDs fabricated on ITO-coated glass substrates. However, if the ITO layer on plastic substrate is deposited by different methods and/or is treated during etching or cleaning processes, the ITO electrical property and surface roughness can be degraded, resulting in poorer OLEDs opto-electronic performances in comparison with the devices on the ITO-coated glass substrate [9],[10].

For the past several years, we have investigated the organic polymer light-emitting devices (PLEDs) on flexible plastic substrates [11][12][13]. The high-quality ITO-coated flexible plastic substrate used in our research is based on polydicylo-pentadiene – "transphan" [14], and is another good substrate candidate for flexible FPDs, along with the previously reported barrier-coated PET plastic substrate [15].

2. Plastic Substrate Properties

The plastic substrate used for PLEDs has a multi-layer structure including the base film of polydicylo-pentadiene – "transphan" with a high-glass transition temperature (T_g~170 °C) and low-birefringence. To enhance the substrate thermal stability, optical characteristics, and gas blocking property, a multi-layer oxygen/moisture barrier (for example, a-SiOx/acrylic/a-SiOx) was deposited on top of the base film. The acrylic and low temperature amorphous silicon oxide can be used as a hard coat and oxygen / moisture barrier, respectively [16],[17],[18]. To further reduce the gas transmission through the substrate, we have added additional PECVD layers, such as a-SiOx:H and a-SiNx:H, on one side of the plastic substrate.

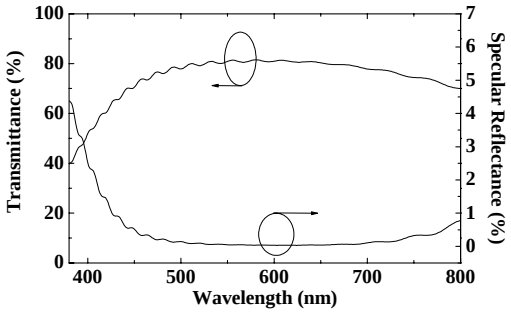

Figure 1. Transmittance and specular reflectance spectra (measured at an incident angle of 7º) of the dry etchable plastic substrate.

On top of the multi-layer substrate, the transparent conducting electrode (TCE-ITO) was defined either by dry etching using a laser-based method [16] or by wet etching. To improve TCE conductivity without significantly affecting the optical transmission through the substrate, a semitransparent thin metal multi-layer (for example, Au/Ag/Au or Ag/Au/Ag) is added between the indium tin oxide (ITO) and metal oxide (ITO or SnO_2) layers. It is well known that a very thin silver or silver containing palladium layer between transparent conducting oxide layers allows a very high electric conductivity, a good mechanical durability, and a high transparency in the visible range due to the anti-reflection effect [19]. Our TCE coating on this plastic substrate has a sheet resistance of 12-13 Ω/□, an optical transmittance of greater than 70% over the visible range, a

specular reflectance of less than 3% over the visible range (figure 1), and an RMS surface roughness of 1.4-2.2 nm over 50 × 50 μm^2.

3. Organic Materials Properties

The light emissive materials used in this work are based on a family of fluorene-containing alternating conjugated copolymers developed by Dow Chemical Corporation. The chemical structures of the materials are described in [20]. Table 1 shows a summary of the materials properties used in this work. The highest occupied molecular orbital (HOMO) and lowest unoccupied molecular orbital (LUMO) levels of different light emissive polymers are obtained from a combination of cyclic voltammetry (CV) and optical spectra. We used this information to construct the energy band diagram of the fabricated devices. The photoluminescence quantum efficiency (PLQE) of the polymers is obtained by the integrating sphere method [21]. The integrated photoluminescence (PL) and electroluminescence (EL) spectra are collected by a JY spectroradiometer system equipped with an integrating sphere as the input optics. From Table 1, we can conclude that the EL spectra of the red, green, and blue materials show similar peak position with slight position shift (<7 nm) in comparison with their PL spectra.

4. Device Opto-electronic Properties

To achieve PLEDs with high efficiency and long lifetime, one basic requirement is needed: balanced electron and hole current, which results from balanced charge injection and transport. The simplest PLED structure consists of a light-emitting layer (LEL) sandwiched between an anode and a cathode. Since the anode/LEL and cathode/LEL junctions have different barrier heights, it is expected that the density of injected holes and electrons will be different. In addition, the injected carriers have different mobilities in the organic polymers. Therefore, when the two types of carriers are injected in the light emissive layer, they do not recombine in identical proportions and the recombination processes take place near the electrode that injects the least mobile carriers. This will lead to a poor efficiency in luminescence because on one hand, a high number of majority carriers reach the opposite electrode without encountering the minority carriers, and on the other hand, a large density of defects near the surface of the injecting electrode will lead to non-radiative recombination.

The multilayer device structure effectively enhances device efficiency by incorporating an electron transport/injection layer (ETL/EIL) between an active emissive layer (EL) and a cathode [22] and/or a hole transport/injection layer (HTL/HIL) between an EL and an anode [23]. Our laboratory has employed the multi-layer device structure to optimize the device efficiency with a careful selection of materials and solvents to avoid damage of the polymer layers during the layer-by-layer, wet spin-coating process. Table 1 shows the device results obtained in our laboratory based on red, green, and blue polymers.

For all studied red, green, and blue polymer devices, the ITO and calcium (Ca) / aluminum (Al) were used as anode and cathode electrodes, respectively. The poly(3,4-ethylene-dioxythiophene) (PEDOT) doped with the poly(styrenesulfonate) (PSS) was used as the hole injection layer (HIL). For red PLEDs, an organic hole transport layer (HTL) is inserted between PEDOT:PSS hole injection (HIL) and light-emissive layer (LEL). Since the highest occupied molecular orbital of the HTL (HOMO~5.3 eV) is located between those of HIL and LEL, the insertion of HTL reduces the effective HOMO level offset between HIL and LEL, reducing the device operation voltage and producing comparable or better device efficiencies in comparison with the conventional PEDOT:PSS-only devices.

Table 1 Summary of material and device properties

	Red	Green	Blue
HOMO (eV)	5.7	5.3	5.8
LUMO (eV)	3.5	2.5	2.3
PLQE	29 ± 5 %	61 ± 5 %	31 ± 5 %
PL peak (nm)	668	547	467
EL peak (nm)	661	549	469
Active layers[a]	HIL/BFE/Red[b]	HIL/Green	HIL/Blue
PE_{max} (lm/W)[c]	0.6	9.9	0.5
EE_{max} (cd/A)[c]	0.7	10	1.7
EQE_{max} (%)[c]	1.5	2.9	1.2
EL CIE[d]	(0.67,0.32)	(0.42,0.56)	(0.17,0.22)

[a] Device structures used for this study is ITO/active layers/Ca/Al

[b] HIL: hole injection layer (PEDOT:PSS), BFE: poly(9, 9'-dioctyl fluorene-2,7-diyl)-co-poly(diphenyl-p-tolyl-amine-4,4'-diyl

[c] PE_{max}, EE_{max}, and EQE_{max} are maximum power efficiency, emission efficiency, and external quantum efficiency, respectively.

[d] EL CIE is the CIE coordinates of the electro-luminescence spectra.

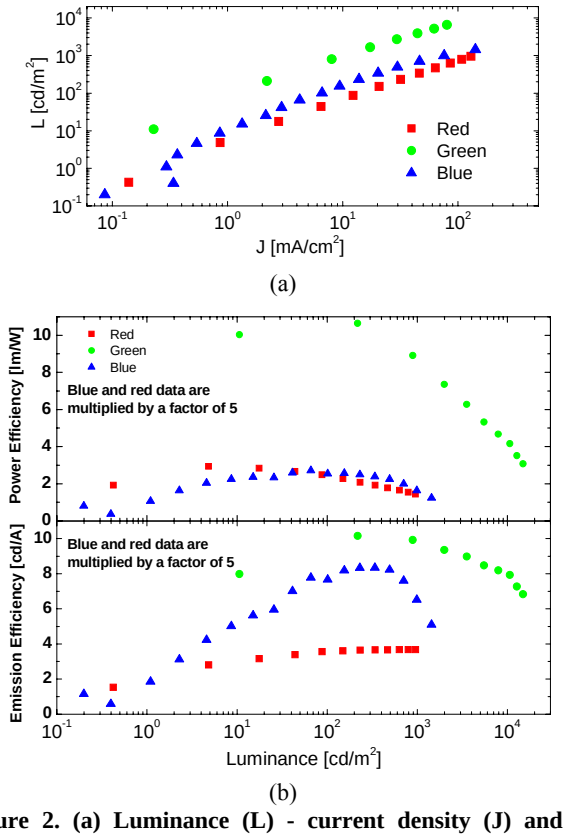

Figure 2. (a) Luminance (L) - current density (J) and (b) Power and emission efficiency versus luminance of the red, green, and blue devices.

Device efficiency and chromaticity are the most important opto-electronic properties of PLEDs. Good device efficiencies were obtained for red, green, and blue PLEDs as shown in figure 2 (b). For the red polymer device, the staircase-like increase of the highest occupied molecular orbital (HOMO) level – reduced effective hole injection (or electron extraction) energy barrier – between anode and LEL enhanced the device efficiencies. For all the PLEDs, a low work function calcium cathode, which reduces the effective electron injection barrier and enhances the device efficiencies, was used. The turn-on voltage, defined at 1 cd/m^2, is ~2.3, ~2.1, and ~5.4 V for red, green and blue devices, respectively.

Figure 3 shows the electroluminescence (EL) spectra for the red, green, and blue PLEDs. We further calculated their corresponding CIE (Commission Internationale de l'Éclairage) color coordinates based on CIE 1931 chromaticity calculations [24]. We achieved the CIE coordinates of the PLEDs in a wide range of the visible spectra when employing different emissive polymers.

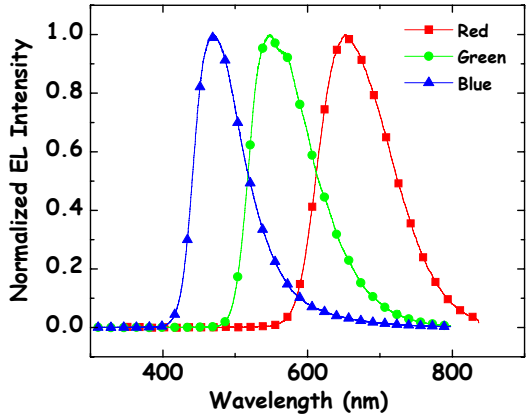

Figure 3. Electroluminescence spectra of the red, green, and blue PLEDs.

5. Angular Distribution of Light Emission

We measured the electroluminescence spectra of the green PLEDs at different angles [25]. From this we concluded that the shape of the measured electroluminescence spectra does not change with the measured angle. We then integrated the spectral radiant intensity over the whole spectra region at each angle and we normalized integrated radiant intensity to its value at the normal angle (θ=0^o) to the plane of the PLED. The variation of the normalized photon density for different angles is shown as curve (b) in figure 4. The experimental light-emission angular distribution of our green PLED is very close to that of a Lambertian light source, in agreement with published results [26]. Also we have obtained the best agreement between experimental and Monte Carlo simulated results when we take into account refractions in the PLED, back-reflection from the cathode, absorption in polymer layers, and interference effect in the ITO thin films. Based on these results we concluded that all effects must be taken into consideration when we compare simulated and experimental PLED opto-electronic characteristics.

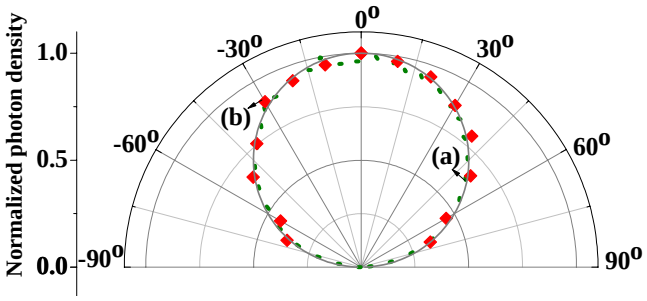

Figure 4. Simulated (a) and experimental (b) angular distribution of the green PLEDs. The background gray solid line represents the Lambertian angular distribution of the light source.

6. PLED SPICE Modeling

Bender et al. proposed an equivalent circuit configuration to describe the injection and bulk limited current in OLED [27]. Bonnassieux et al. reported an OLED SPICE (Simulation Program with Integrated Circuit Emphasis) model in the passive matrix configuration with the consideration of electrical coupling of the pixels [28]. We have also used an engineering circuit model to simulate the current density – voltage (J-V) characteristics of PLEDs.

Since the J-V characteristics of our PLEDs are limited by both carrier injection at polymer-electrode interface and conduction in polymer thin films [29], the J-V characteristics could not be simply described by a single diode behavior. Three parallel-connected diodes (D_1, D_2 and D_3) with serial resistors (R_1, R_2 and R_3), parallel resistor R_P, and capacitor C_P need to be considered to accurately fit the PLED experimental J-V curves (figure 5).

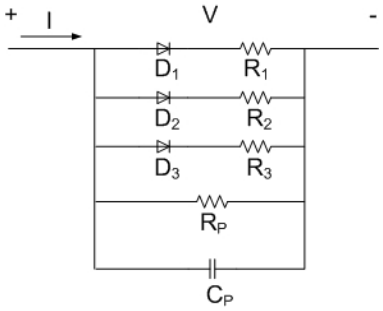

Figure 5. Proposed equivalent circuit model for a green PLED.

We used the following diode current equation:

$$J = J_s\left(e^{qV_a/Nk_BT} - 1\right)$$

where J_s is the reverse saturation current of the diode, q is the elemental charge, V_a is the applied bias, N is an ideality factor, k_B is the Boltzmann constant, and T is temperature. For our simulation (figure 6), the fitting parameters for a green PLED are: D_1 (J_S = 3.0e-8 A, N = 3.1), D_2 (J_S = 3.0e-14 A, N = 4.5), D_3 (J_S = 1.0e-20 A, N = 3.9), R_1=16.4 Ω, R_2=60 Ω, R_3=400 KΩ, and R_P=10 MΩ. To perform the simulation of transient response of PLEDs, a parallel capacitor is also needed. The capacitance value of a PLED

is measured to be 1.1 nF at a frequency of 10 kHz for a PLED size of 6 mm^2. For PLEDs operated in the low voltage regime (before turn on), the current mainly flows through the parallel connected diode D_1. After PLED is turned on, D_2 dominates the J-V characteristics. For PLED operated in the high voltage regime, D_3 dominates the J-V characteristic while the current contributions flowing through D_1 and D_2 are negligible.

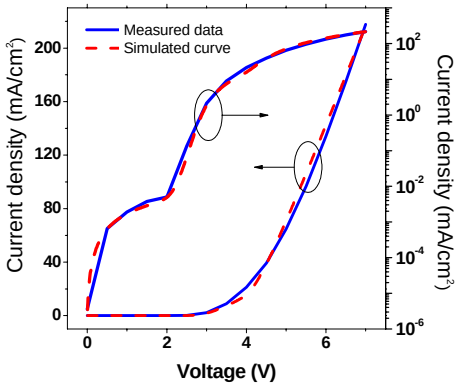

Figure 6. Experimental and simulated J-V characteristics of a green PLED.

6. Conclusions

We reported on the opto-electronic properties of red, green, and blue poly (fluorene) co-polymer light-emitting devices (PLEDs) fabricated on a flexible plastic substrate having a water vapor and oxygen transmission rate of less than 10^{-5} g/cm^2-day-atm and 10^{-7} cc/cm^2-day-atm, respectively. We obtained a wide range of color gamut and a maximum emission efficiency of 0.7, 10, and 1.7 cd/A for red, green, and blue PLEDs, respectively. Finally, a simple SPICE equivalent circuit model was proposed to simulate the PLED current density-voltage characteristics.

7. Acknowledgment

The authors would like to thank Mr. Aaron Johnson for the measurement of CV data of blue material and Mr. Hojin Lee for the measurement of the photoluminescence spectra of the blue material. This work was supported by NIH and DARPA grants.

8. Reference

1 J. J. Brown and G. Yu, SID Tech. Dig., 34, 855 (2003).

2. A. Sugimoto, H. Ochi, S. Fujimura, A. Yoshida, T. Miyadera, and M. Tsuchida, IEEE J. Selected Topics Quantum Electron., 10, 107 (2004).

3 A. B. Chwang, M. A. Rothman, S. Y. Mao, R. H. Hewitt, M. S. Weaver, J. A. Silvernail, K. Rajan, M. Hack, J. J. Brown, X. Chu, L. Moro, T. Krajewski, and N. Rutherford, Appl. Phys. Lett., 83, 413 (2003).

4 S. Utsunomiya, T. Kamakura, M. Kasuga, M. Kimura, W. Miyazawa, S. Inoue, and T. Shimoda, SID Tech. Dig., 34, 864 (2003).

5 J. S. Lewis and M. S. Weaver, IEEE J. Select Topics Quantum Electron., 10, 45 (2004).

6 G. Gustafsson, Y. Cao, G.M. Treacy, F. Kavetter, N. Colaneri, and A.J. Heeger, Nature, 357, 477 (1992).

7 G. Gu, P.E. Burrows, S. Venkatesh, S.R. Forrest, and M.E. Thompson, Optics Letters, 22, 172 (1997).

8 H. Lim, W.J. Cho, C.S. Ha, S. Ando, Y.K. Kim, C.H. Park, and K. Lee, Advanced Materials, 14, 1275 (2002).

9 J. Zhao, S. Xie, S. Han, Z. Yang, L. Ye, and T. Yang, Phys. Stat. Sol. A, 184, 233 (2001).

10 S.H. Kwon, S.Y. Paik, and J.S. Yoo, Synthetic Metals, 130, 55 (2002).

11 Y. Hong, Z. Hong and J. Kanicki, Proc. SPIE, 4105, 356 (2000).

12 Y. Hong, Z. He, S. J. Lee, and J. Kanicki, Proc. SPIE, 4464, 329 (2001).

13 Y. He and J. Kanicki, Appl. Phys. Lett., 76, 661 (2000).

14 Y. Hong, Z. He, N. S. Lennhoff, D. A. Banach, and J. Kanicki, Journal Electron. Mater., 33, 312 (2004).

15 P.E. Burrows, G.L. Graff, M.E. Gross, P.M. Martin, M.K. Shi, M. Hall, E. Mast, C. Bonham, W. Bennett, and M.B. Sullivan, Displays, 22, 65 (2001).

16 H.C. Choi, Y.Z. Chu, L.S. Heath, W.K. Smyth, US Patent #6,379,509 (30 April 2002).

17 N.S. Lennhoff and J. Ram, US Patent Application #20020182386.

18 P.Y.Z. Chu, H.C. Choi, L.S. Heath, C.S. Ko, J. Mack, P. Nagarkar, J. Richard, W. Smyth, T. Wang, Proc. of SID '98, 1099 (1998).

19 Y. Aoshima, M. Miyazaki, K. Sato, Y. kao, S. Takaki, K. Adachi, Jpn. J. Appl. Phys., 40, 4166 (2001).

20 M. T. Bernius, M. Inbasekaran, J. O'Brien, and W. Wu, Adv. Mater., 12, 1737 (2000).

21 J. C. de Mello, H. F. Wittmann, and R. H. Friend, Adv. Mater., 9, 230 (1997).

22. C. Adachi, T. Tsutsui, S. Saito, Appl. Phys. Lett., 55, 1489 (1989).

23. N. C. Greenham, S. C. Moratti, D. D. C. Bradley, R. H. Friend, A. B. Holmes, Nature, 365, 628 (1993).

24. J. W. T. Walsh, Photometry, Constable and Company Ltd., London, 321 (1953).

25 S. J. Lee, A. Badano, and J. Kanicki, IEEE J. of Selected Topics in Quantum Electron., 10, 37 (2004).

26 N. C. Greenham, R. H. Friend, and D. D. C. Bradley, Adv. Mater., 6, 491 (1994).

27 J. P. Bender, B. J. Norris and J. F. Wager, "OLED modeling via spice," http://eecs.oregonstate.edu/matdev/pub.html

28 Y. Bonnassieux and D. B. Van, IDRC, 30, (2003).

29 V. Bulovic and S. R. Forrest, in Semiconductors and Semimetals, Academic Press, 65, 11 (2000).